Available online at www.sciencedirect.com
SCIENCE DIRECT®
Journal of Crystal Growth 268 (2004) 590–595
JOURNAL OF CRYSTAL GROWTH
www.elsevier.com/locate/jcrysgro

Investigation of individual CuO nanorods by polarized micro-Raman scattering

T. Yu[a], X. Zhao[a], Z.X. Shen[a,*], Y.H. Wu[b,c], W.H. Su[d]

[a] *Physics Department, Faculty of Science, National University of Singapore, 2 Science Drive 3, Singapore 117542, Singapore*
[b] *Department of Electrical and Engineering, National University of Singapore, Singapore 117576, Singapore*
[c] *Data Storage Institute, 5 Engineering Drive 1, Singapore 117608, Singapore*
[d] *Physics Department, Harbin Institute of Technology, Harbin, China*

Abstract

Rod-shaped CuO nanostructures were successfully synthesized by a one-step annealing process in air using copper plates as starting material. Phase analysis was carried out using X-ray diffraction, transmission electron microscopy and micro-Raman scattering and the results confirmed the nanorods as single-phase CuO. For the first time, single individual CuO nanorods with different aspect ratios were investigated by polarized micro-Raman scattering in this work. An obvious anisotropy in the intensity of Raman modes was observed when the electric field vector of the incident laser beam is parallel and perpendicular to the long axis of a nanorod. The mechanism responsible for the observed polarized Raman spectra was attributed to the polarization effect produced by the large length to diameter ratio of the nanorods and the large dielectric contrast between these nanorods and their surrounding environment.

PACS: 63.22.+m; 78.67.-n; 81.07.-6; 74.25.Kc

Keywords: A1. Polarized Raman scattering; B1. Cupric oxide; B1. Individual nanorod

1. Introduction

Recently, quasi one-dimensional (1-D) solid nanostructures (nanowires/nanorods) have attracted much attention for both fundamental and practical reasons. Compared with micrometer-sized whiskers and fibers, 1-D nanostructures are expected to exhibit remarkable optical, electrical, magnetic, and mechanical properties. Many methods have been developed to prepare such nanostructures, i.e. vapor–liquid–solid (VLS) growth [1–3], solution–liquid–solid (SLS) method [4], template-mediated growth [5], electron-beam lithography (EBL) [6] and scanning tunneling microscopy (STM) [7]. As a p-type semiconductor with a narrow band gap (1.2 eV) and the basic building block of several high-temperature superconductors, cupric oxide (CuO) has generated renewed interest. It can be used in a wide range of applications such as gas sensor [8], magnetic storage media [9], solar-energy transformation [10], electronics [11], semiconductors [12], varistors

*Corresponding author. Tel.: +65-6874-6390; fax: +65-6777-6126.
E-mail address: physzx@nus.edu.sg (Z.X. Shen).

0022-0248/$ - see front matter © 2004 Elsevier B.V. All rights reserved.
doi:10.1016/j.jcrysgro.2004.04.097

[13], and catalysis [14]. Moreover, CuO nanostructured materials have attractive photothermal and photoconductive properties [15]. Different approaches have been used for the synthesis of CuO nanoparticles and films. One-dimensional CuO nanostructure (nanowires/nanorods) has been successfully synthesized by thermal decomposition of CuC_2O_4 precursor [16], oxidation of Cu substrates [17], and wet-chemical route [18]. The successful preparation of CuO nanowires/nanorods is believed to enrich our understanding of its fundamental properties, which may lead to enhancement of performance in its applications.

Raman spectra are normally determined by the crystal structure of the sample and the relative orientation between its crystal axes and the polarization direction of the incident laser. However, when the size of the sample is smaller than the focus spot of the laser, the shape of the sample also becomes a contributing factor to the Raman spectra because the effective electric field inside the sample can be very different along different directions due to polarization for samples with a large length to diameter ratio. Contribution from both the single crystal property and the sample geometry has to be accounted for properly in the Raman study of nanoparticles, such as nanorods and nanotubes that show a large polarization. Raman spectroscopy has played a unique and significant role in the study of 1-D nanostructures, e.g. carbon nanotubes [19–21]. However, no polarized Raman scattering has been used to investigate individual CuO nanorods. In this work, we present the first polarized Raman scattering study of individual free-standing single-crystal CuO nanorods synthesized by thermal treatment of copper plate. Our results show that the Raman peak intensities are dominated by the polarization resulted from the shape of the nanorods, i.e. the large length to diameter ratio.

2. Experimental procedure

A 1 cm × 1 cm piece of commercial copper plate (99.999% purity, Sigma-Aldrich Pte. Ltd.) was first rinsed by acetone followed by de-ionized water several times. After it had been dried using an air gun, the Cu plate was annealed at 400°C for 24 h in air. CuO nanorods were contained in the black ash-like top layer formed on the Cu plate. This black layer was peeled off carefully and characterized by X-ray diffraction (XRD), scanning electron microscopy (SEM) and transmission electron microscopy (TEM). In order to perform the polarized Raman scattering study on an isolated free-standing nanorod, a small amount of as-annealed black pieces was ground slightly and suspended in de-ionized water. After 30-min ultrasonic agitation, the suspension was dispread onto a quartz substrate for Raman measurement. Under low magnification TEM or optical microscope used in micro-Raman experiments, Cu_2O appears as small flakes and CuO as rods of several micrometer in length. When dispersed on quartz slides, they can be easily identified and studied separately by micro-Raman spectroscopy. All micro-Raman spectra were measured in the back-scattering geometry using a Renishaw Ramascope System 2000 with an Olympus microscope attachment. The 514 nm line of an argon-ion laser was used as the excitation source.

3. Results and discussion

Fig. 1 shows the XRD pattern of the as-annealed black ash, where, same as reported in Ref. [17], both Cu_2O and CuO phases are present. The Cu_2O exists as a thin film precursor for growing CuO nanorods during the oxidation of Cu plate [17]. Our TEM and Raman results also demonstrate that the nanorods formed in this top layer are crystalline phase CuO. A typical TEM morphology of the as-synthesized product was shown in Fig. 2a. It can be seen that the diameters of nanorods vary from about 20 to 150 nm and the lengths are several micrometers. The vapor–solid (VS) mechanism for the growth of CuO nanorods is also clearly demonstrated by the existence of the conical tip at the end of nanorods, instead of particle-type terminations, which is a most remarkable sign of the VLS growth mechanism [16,17]. Fig. 2b displays the high-resolution TEM image of a nanorod. It is shown that the nanorod formed in this work has a single crystal property.

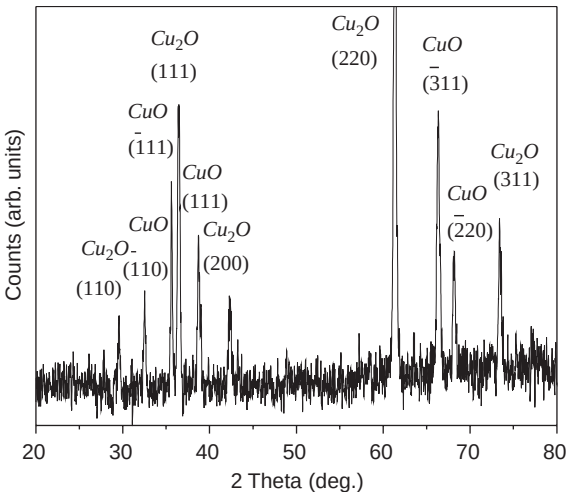

Fig. 1. XRD pattern of the black top layer of the Cu plate after annealing at 400°C for 24 h, showing both CuO and Cu_2O phases.

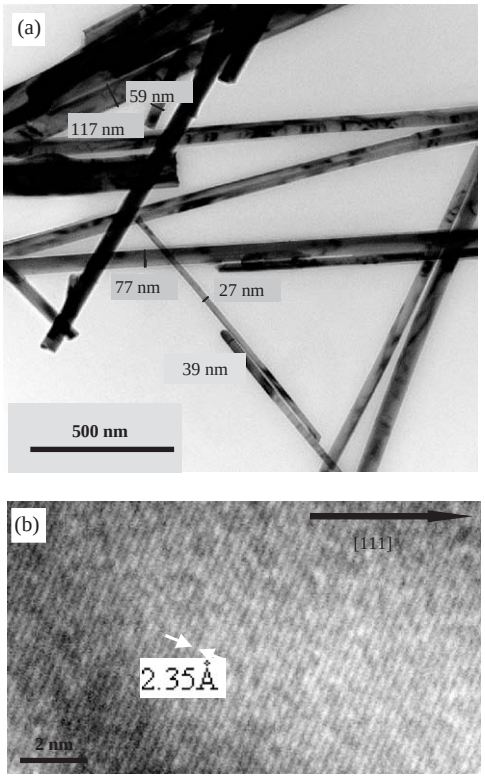

Fig. 2. TEM image of CuO nanorods. (a) Morphologies of the as-prepared CuO nanorods. (b) HRTEM image of a single CuO nanorod showing its crystalline property.

The spacing between the diffraction planes was measured to be 2.35 Å, which corresponds well with the spacing between (1 1 1) planes ($d_{111} = 2.32$ Å) in monoclinic CuO [22]. The angle between the (1 1 1) plane and the long axis of CuO nanorod (indicated by an arrow in Fig. 2b) was measured to be about 66.8°. This angle matches well the value of 67.2° between the (1 1 1) plane and the [1 1 1] crystal axis, indicating that the growth direction of our CuO nanorod is [1 1 1]. This is consistent with previous studies [17,18].

CuO has a monoclinic structure with a space group symmetry of C_{2h}^6 [23]. There are twelve zone-center optical-phonon modes, $4A_u + 5B_u + A_g + 2B_g$, three of which $A_g + 2B_g$ are Raman active [24]. In this work, all the Raman spectra were recorded under the backscattering geometry. In a typical experiment, the long axis and the length of the nanorod were identified using the microscope attached to the Raman system and the diameter of the nanorod was determined by SEM. The angle θ between the long axis of the CuO nanorod and the polarization direction of the incident laser is adjusted between 0° and 180° using a half-wave plate (see Fig. 3, inset). Typical Raman spectra of the CuO nanorod as a function of θ are shown in Fig. 3. Three peaks at 295.2,

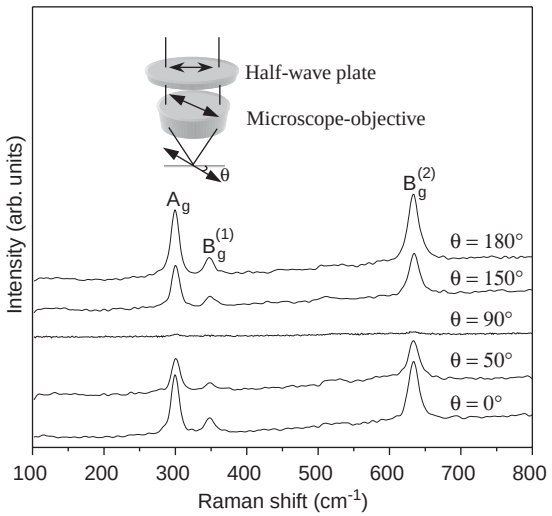

Fig. 3. Typical Raman spectra of an isolated CuO nanorod at several angles, where the diagram shows the experimental geometry of the Raman scattering measurement.

342.7 and 633.5 cm^{-1}, correspond to the A_g (296 cm^{-1}), $B_g^{(1)}$ (346 cm^{-1}), and $B_g^{(2)}$ (636 cm^{-1}) modes of bulk CuO crystals [25], respectively. No Cu_2O modes [26] are present, demonstrating the single phase property of our CuO nanorods. Due to the relatively large diameter (average diameter: 65 nm) of the nanorod samples, quantum confinement effects such as the dramatic down shift and broadening of Raman peaks [18] were not observed in this work. It is noteworthy that all the modes exhibit strong polarization dependence demonstrated by the obvious variation of peak intensity with angle θ.

As mentioned in the Introduction, the Raman spectra of a nanorod sample are governed by the geometry of the sample as well as its crystal structure. In this study, we try to distinguish which is the dominant factor in determining the Raman spectra observed in our individual CuO nanorod experiments. We have fitted the intensity of the A_g mode and the two B_g modes using least-squares fit with Lorentzian line-shape and Fig. 4 presents the fitting results as a function of θ. It is obvious that all the modes display a polarization dependence with a period of 180°. Most importantly, all the modes, regardless A_g or B_g modes, are strongest when the polarization direction of the incident laser is parallel to the long axis of the nanorod ($\theta = 0°$ or 180°) and weakest in perpendicular geometry ($\theta = 90°$). As we will show below, this clearly demonstrates that the Raman spectra are mainly determined by the geometry of the sample and not its single crystal property.

Chen et al. [25] and Goldstein et al. [27] systematically investigated the intrinsic polarization dependence of Raman modes for bulk CuO single crystals. The strongest polarization direction of A_g mode was predicted to be along the [1 1 $\bar{2}$] crystal axis [25] and it was experimentally observed at $150° \pm 5°$ with respect to the [0 0 1] axis [27]. The two results are consistent since the angle between the [1 1 $\bar{2}$] and [0 0 1] directions is 152.6°. The above results do not agree with our result with nanorod samples where the A_g mode is strongest when the electric vector of the laser is parallel to the long axis of the nanorods, i.e. the [1 1 1] crystal axis, which makes a 78° angle with the [1 1 $\bar{2}$] axis. Moreover, from the Raman tensors, the A_g and

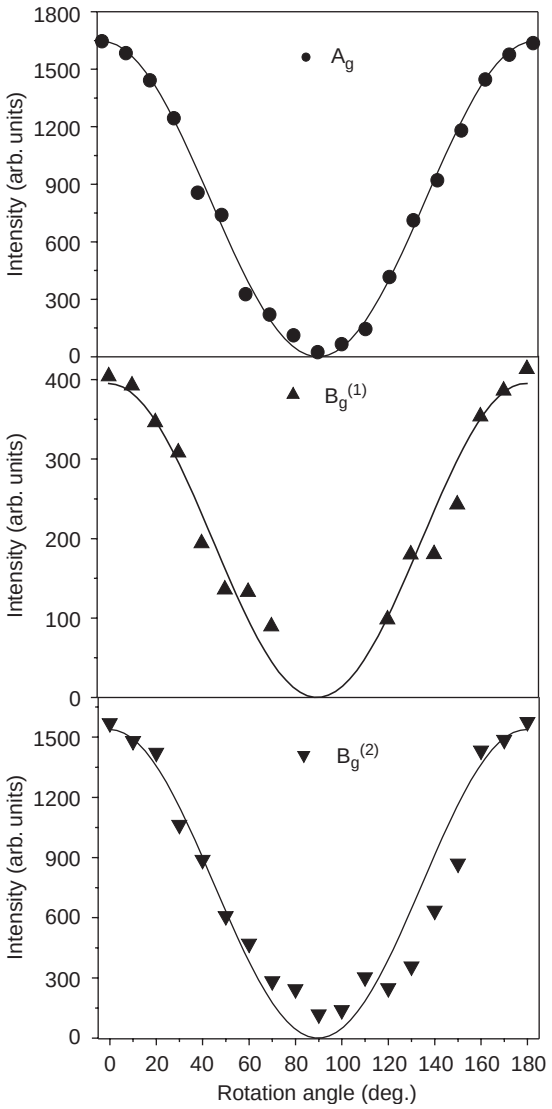

Fig. 4. Intensity of the three Raman modes as a function of the angle θ, between the polarization direction of the incident laser and the long axis of nanorod. The symbols are experimental data and the solid curves are fitted results using $\cos^2\theta$ functions. Note that all the Raman modes show a maximum intensity at $\theta = 0°$ and minimum intensity at $\theta = 90°$, which agrees with predictions by the "sample geometry" model.

two B_g modes of bulk single crystal CuO have different polarization dependence as observed by Chen et al. [25], instead of the same θ dependence observed in this work (see Fig. 3). Hence, the Raman spectra observed in our CuO nanorod

samples cannot be explained by the intrinsic properties of single crystal.

From the classical electromagnetic theory, the electric field inside a 1-D nanostructure which has a large length to width ratio and width smaller than the wavelength of laser beam could be dramatically attenuated when the incident laser is polarized perpendicular to the long axis of the nanorods:

$$E_i = \frac{2\varepsilon_0}{\varepsilon + \varepsilon_0} E_e \quad (1)$$

where E_i is the electric field inside the nanorods, E_e the excitation field, and $\varepsilon(\varepsilon_0)$ is the dielectric constant of the nanorod (vacuum) [28]. On the other hand, the electric field inside is the same as that of the incident field in the direction parallel to the nanorod. When $\varepsilon \gg \varepsilon_0$ ($\varepsilon_{CuO} = 18.1$ [29]), the electric field perpendicular to the long axis is negligible and the intensities of all Raman peaks are determined by the electric field component along the long axis, which has a $\cos\theta$ dependence on the angle θ shown in Fig. 3. Hence, the peak intensities show a $\cos^2\theta$ dependence with maximum at $\theta = 0^\circ$. Fig. 4 plots the fitted curves using a $\cos^2\theta$ function and the fitting results show good agreement with experimental data for all three Raman modes despite their different θ dependence predicted based on their Raman tensors. Therefore, our results show that the Raman spectra of CuO nanorods are dominated by the large length to diameter ratio of the samples and the large dielectric contrast between these nanorods and air. Similar polarization dependence were also observed in polarized Raman scattering study of isolated single-wall carbon nanotubes (SWNTs) [30] and photoluminescence investigation of individual InP nanowire [31], where both types of 1-D nanostructures show a large length to diameter ratio.

In conclusion, polarized micro-Raman scattering experiments have been performed on isolated free-standing CuO nanorods synthesized by heating a Cu plate in air. Different from bulk single crystals, the polarization dependence of Raman modes in free-standing CuO nanorods is dominated by the adjustment of the electric filed inside nanorods due to the large length to diameter ratio and big dielectric contrast between these nanorods and their surroundings.

References

[1] A.M. Morales, C.M. Lieber, Science 279 (1998) 208.
[2] H.Z. Zhang, D.P. Yu, Y. Ding, Z.G. Bai, Q.L. Hang, S.Q. Feng, Appl. Phys. Lett. 73 (1998) 3396.
[3] Y.Q. Zhu, W.B. Hu, W.K. Hsu, M. Terrones, N. Grobert, T. Karali, H. Terrones, J.P. Hare, P.D. Townsend, H.W. Kroto, D.R.M. Walton, Adv. Mater. 11 (1999) 844.
[4] T.J. Trentler, K.M. Hickman, S.C. Geol, A.M. Viano, P.C. Gibbons, W.E. Buhro, Science 270 (1999) 1791.
[5] H. Dai, E.W. Wong, Y.Z. Yu, S.S. Fan, C.M. Lieber, Nature 375 (1999) 769.
[6] E. Leobandung, L. Guo, Y. Wang, S.Y. Chou, Appl. Phys. Lett. 67 (1997) 938.
[7] T. One, H. Saitoh, M. Esashi, Appl. Phys. Lett. 70 (1997) 1852.
[8] P. Poizot, S. Laruelle, S. Grugeon, L. Dupont, J.M. Taracon, Nature 407 (2000) 496.
[9] R.V. Kumar, Y. Diamant, A. Gedanken, Chem. Mater. 12 (2) (2000) 301.
[10] H. Cao, S.L. Suib, J. Am. Chem. Soc. 116 (1994) 5334.
[11] B. Ao, L. Kummerl, D. Haarer, Adv. Mater. 7 (1995) 495.
[12] M. Singhal, P. Chhabra, P. Kang, D.O. Shah, Mater. Res. Bull. 32 (1997) 233.
[13] Y. Jiang, S. Decker, C. Mohs, K.J. Klabunde, J. Catal. 180 (1998) 24.
[14] T. Ishihara, M. Higuchi, T. Takagi, M. Ito, H. Nishiguchi, T. Takita, J. Mater. Chem. 8 (1998) 2037.
[15] A.E. Rakhshni, Solid State Electron. 29 (1986) 7.
[16] C.K. Xu, Y.K. Liu, G.D. Xu, G.H. Wang, Mater. Res. Bull. 37 (2002) 2365.
[17] X.C. Jiang, T. Herricks, Y.N. Xia, Nano Lett. 2 (2002) 1333.
[18] W. Wang, Z. Liu, Y. Liu, C. Xu, C. Zheng, G. Wang, Appl. Phys. A 76 (2003) 417.
[19] A.M. Rao, P.C. Eklund, S. Bandow, A. Thess, R.E. Smalley, Nature 388 (1997) 257.
[20] J. Chen, M.A. Hamon, H. Hu, Y.S. Chen, A.M. Rao, P.C. Eklund, R.C. Haddon, Science 282 (1998) 95.
[21] A.M. Rao, E. Richter, S. Bandow, B. Chase, P.C. Eklund, K.A. Williams, S. Fang, K.R. Subbaswamy, M. Menon, A. Thess, R.E. Smalley, G. Dresselhaus, M.S. Dresselhaus, Science 275 (1997) 187.
[22] Joint Committee on Powder Diffraction Standards. Diffraction Data File, No. 45-0937, International Centre for Diffraction Data (ICDD, formerly JCPDS), Newtown Square, PA, 1991.
[23] S. Asbrink, L.J. Norrby, Acta Crystallogr. Sec. B 26 (1970) 8.
[24] J. Chrzanowski, J.C. Irwin, Solid State Commun. 70 (1989) 11.
[25] X.K. Chen, J.C. Irwin, J.P. Franck, Phys. Rev. B 52 (1995) R13130.

[26] K. Reimann, K. Syassen, Phys. Rev. B 39 (1989) 11113.
[27] H.F. Goldstein, D.S. Kim, P.Y. Yu, L.C. Bourne, Phys. Rev. B 41 (1990) 7192.
[28] L.D. Landu, E.M. Lifshitz, L.P. Pitaevskii, Electrodynamics of Continuous Media, Pergamon, Oxford, 1984, pp. 34–42.
[29] CRD Handbook of Chemistry and Physics, 83rd Edition, CRC Press, Boca Raton, FL, 2002–2003, pp. 12–15.
[30] G.S. Duesberg, I. Loa, M. Burghard, K. Syassen, S. Roth, Phys. Rev. Lett. 85 (2000) 5436.
[31] J.F. Wang, M.S. Gudiksen, X.F. Duan, Y. Cui, C.M. Lieber, Science 293 (2001) 1455.